mTOR Regulates Endocytosis and Nutrient Transport in Proximal Tubular Cells

Florian Grahammer,* Suresh K. Ramakrishnan,[†] Markus M. Rinschen,[‡] Alexey A. Larionov,[†] Maryam Syed,[†] Hazim Khatib,[§] Malte Roerden,[§] Jörn Oliver Sass,[‖¶] Martin Helmstaedter,* Dorothea Osenberg,* Lucas Kühne,* Oliver Kretz,* Nicola Wanner,* Francois Jouret,** Thomas Benzing,[‡] Ferruh Artunc,[§] Tobias B. Huber,*[††‡‡] and Franziska Theilig[†]

*Department of Medicine IV, Medical Center—University of Freiburg, Faculty of Medicine, University of Freiburg, Freiburg, Germany; [†]Institute of Anatomy, Department of Medicine, University of Fribourg, Fribourg, Switzerland; [‡]Department II of Internal Medicine and Center for Molecular Medicine Cologne, University of Cologne, Cologne, Germany; [§]Department of Medical IV, Sektion Nieren- und Hochdruckkrankheiten, University of Tübingen, Tübingen, Germany; [‖]Bioanalytics and Biochemistry, Department of Natural Sciences, Bonn Rhein Sieg University of Applied Sciences, Rheinbach, Germany; [¶]Division of Clinical Chemistry and Biochemistry and Children's Research Centre, University Children's Hospital Zürich, Zurich, Switzerland; **Groupe Interdisciplinaire de Génoprotéomique Appliquée, Cardiovascular Sciences, University of Liège, Liege, Belgium; and [††]BIOSS, Centre for Biological Signalling Studies and [‡‡]FRIAS, Freiburg Institute for Advanced Studies and ZBSA, Center for Biological System Analysis, Albert Ludwigs University of Freiburg, Freiburg, Germany

ABSTRACT

Renal proximal tubular cells constantly recycle nutrients to ensure minimal loss of vital substrates into the urine. Although most of the transport mechanisms have been discovered at the molecular level, little is known about the factors regulating these processes. Here, we show that mTORC1 and mTORC2 specifically and synergistically regulate PTC endocytosis and transport processes. Using a conditional mouse genetic approach to disable nonredundant subunits of mTORC1, mTORC2, or both, we showed that mice lacking mTORC1 or mTORC1/mTORC2 but not mTORC2 alone develop a Fanconi-like syndrome of glucosuria, phosphaturia, aminoaciduria, low molecular weight proteinuria, and albuminuria. Interestingly, proteomics and phosphoproteomics of freshly isolated kidney cortex identified either reduced expression or loss of phosphorylation at critical residues of different classes of specific transport proteins. Functionally, this resulted in reduced nutrient transport and a profound perturbation of the endocytic machinery, despite preserved absolute expression of the main scavenger receptors, MEGALIN and CUBILIN. Our findings highlight a novel mTOR–dependent regulatory network for nutrient transport in renal proximal tubular cells.

With the transition from water to land, mammalian kidneys developed into a high–pressure filtration system combining excess ultrafiltration with highly efficient tubular reabsorption to minimize nutrient and protein loss.[1] The vast amount of the ultrafiltrate (approximately 60%–70%), including virtually all nutrients, is already being reabsorbed by the first nephron segment, the proximal tubule (PT).[2] Specific loss of PT amino acid or phosphate transport function is associated with genetically defined disease entities, such as Hartnup disorder or hypophosphatemic rickets.[3,4] In contrast, disrupted energy metabolism or toxic injury can simultaneously affect several transport systems, leading to a Fanconi syndrome.[5,6] In addition to aminoaciduria,

glucosuria, and phosphaturia, Fanconi syndrome is characterized by low molecular weight proteinuria.[7] This is caused by dysfunction of receptor-mediated endocytosis, which is mediated by the two scavenger receptors, MEGALIN and CUBILIN, followed by clathrin-mediated internalization of the ligand-receptor complex.[8] Fusion with early endosomes delivers the complex to the endosomal-lysosomal compartment, leading to recycling or degradation of retrieved proteins.[8] The prominent endocytotic activity of the PT is important to retrieve vital plasma proteins and maintain body homeostasis.[9] Although individual components of this system have been recently described, little is known on the organ-specific regulation of these transport processes.

The mammalian homolog of TOR1 (mTORC1) and mTORC2 are intracellular multiprotein complexes regulating tissue–specific cellular functions.[10] The regulatory associated protein of mammalian target of rapamycin (RAPTOR) is important to assemble mammalian target of rapamycin (mTOR) complex 1, and its function can be blocked by rapamycin. In contrast, mTORC2, containing the rapamycin-insensitive companion of mammalian target of rapamycin (RICTOR) as a scaffolding protein, seems to be insensitive to short–term rapamycin treatment.[11] mTORC1 integrates a wide variety of signals, including growth factors, amino acids, cellular energy content, and cellular stress, to regulate cellular growth and division as well as lipid and mitochondrial biogenesis.[12,13] The wide range of mTORC1 phosphorylation targets is still incompletely defined but seems to vary in a cell-specific manner. Conversely, mTORC2 seems to be activated by insulin and related pathways and controls several downstream AGC kinases by phosphorylating their hydrophobic motif.[14,15] Thereby, mTORC2 could play an important role in cell survival and organization of the cytoskeleton.

To investigate the effect of mTOR-controlled signaling in PT function, we generated inducible conditional *Raptor, Rictor,* or double-knockout mice in renal tubular cells along the nephron.

RESULTS

Loss of mTOR in PT Cells Results in a Fanconi-Like Phenotype

Expression of the mTORC1 and mTORC2 complexes in the PT was verified by staining for mTOR, RAPTOR, S6K1, ribosomal S6 protein (S6P), and *N*-Myc Downstream Regulated 1 (NDRG1) (Supplemental Figure 1). All components were strongly expressed in the S1 and S2 segments of the PT in either overlay or close vicinity to MEGALIN. The proximal tubular S3 segment only showed minor signal intensity for mTOR, S6K1, and S6P and was devoid of signals for RAPTOR and NDRG1. To examine the effects of mTORC deletion on PT function, we generated mice with doxycycline–inducible *Pax8* promotor–driven tubular deletion of *Raptor* (*Raptorfl/fl × Pax8rtTA × TetOCre*; subsequently termed Rap$^{\Delta Tubule}$), *Rictor* (*Rictorfl/fl × Pax8rtTA × TetOCre*; subsequently termed Ric$^{\Delta Tubule}$), or both

genes (*Raptorfl/fl × Rictorfl/fl × Pax8rtTA × TetOCre*; subsequently termed RapRic$^{\Delta Tubule}$) (Figure 1, A–C). Protein abundance or reduced phosphorylation of known downstream targets was used to assess efficiency of our knockout approach (Figure 1, D–F). In comparison with the respective control group, all examined parameters were at least reduced by 70% (Rap$^{\Delta Tubule}$: RAPTOR, $-74.6\%\pm4.6\%$; p-S6P/S6P, $-78.9\%\pm6.4\%$; $P<0.05$; $n=6$; Ric$^{\Delta Tubule}$: RICTOR, $-84.5\%\pm8.4\%$; p-NDRG1/NDRG1, $-71.1\%\pm3.7\%$; $P<0.05$; $n=6$; RapRic$^{\Delta Tubule}$: RAPTOR, $-78.3\%\pm6.2\%$; RICTOR, $-69.1\%\pm5.3\%$; p-S6P/S6P, $-89.2\%\pm4.7\%$; p-NDRG1/NDRG1, $-71.7\%\pm9.8\%$; $P<0.05$; $n=6$) (Figure 1, D–F).

Measurement of urinary glucose and phosphate excretion in RapRic$^{\Delta Tubule}$ mice revealed 3.3- and fivefold increases in urinary losses of glucose and phosphate, respectively, indicating impaired nutrient reabsorption (Figure 1H). In addition, SDS-PAGE of urinary samples revealed a slight increase in albuminuria in Rap$^{\Delta Tubule}$, which was significant in RapRic$^{\Delta Tubule}$ (Figure 1, I and K). This observation was confirmed by direct measurement of mouse albumin in urinary samples (Figure 1L). Furthermore, an increase in low molecular mass (LMW) proteinuria between 25 and 68 kD could be detected in RapRic$^{\Delta Tubule}$ ($+126\%\pm37\%$; $P<0.05$; $n=5$) as well as a significant increase in proteinuria at approximately 25 kD in Rap$^{\Delta Tubule}$ and RapRic$^{\Delta Tubule}$ animals (Rap$^{\Delta Tubule}$: $+70\%\pm13\%$; RapRic$^{\Delta Tubule}$: $+44\%\pm6\%$; $P<0.05$; $n=5$). In addition, a pronounced increase in urinary amino acid excretion was observed in Rap$^{\Delta Tubule}$ animals, and an even more pronounced increase was in RapRic$^{\Delta Tubule}$ animals but not in Ric$^{\Delta Tubule}$ mice (Figure 1M, Supplemental Figure 2A). Amino acid plasma concentrations were similar in all experimental groups (Supplemental Figure 2B), confirming a renal amino acid transport defect rather than defects in hepatic or muscular metabolism.

Compared with control mice, Rap$^{\Delta Tubule}$ and RapRic$^{\Delta Tubule}$ animals showed significantly higher food and fluid intakes, which were associated with increased urinary volume and sodium excretion (Supplemental Table 1). No alterations were found in Ric$^{\Delta Tubule}$ animals. Together, these data show a significant mTORC1–dependent defect in tubular reabsorption of glucose, phosphate, amino acids, LMW proteins, and albumin.

mTOR Regulates PTC Endocytosis and Intracellular Trafficking *In Vivo*

To gain additional insights into the effects of gene knockout on PT endocytosis, mice were injected with horseradish peroxidase (taken up by fluid-phase endocytosis) and Alexa555-coupled lactoglobulin (reabsorbed by receptor-mediated endocytosis) before perfusion fixation.[16] Morphologic analysis revealed a strong reduction of fluid-phase endocytosis in Rap$^{\Delta Tubule}$ and RapRic$^{\Delta Tubule}$ animals, whereas no change was observed in Ric$^{\Delta Tubule}$ mice (Figure 2A). Similarly, confocal microscopy analysis showed a reduced receptor–mediated endocytosis in Rap$^{\Delta Tubule}$ and RapRic$^{\Delta Tubule}$ mice in comparison
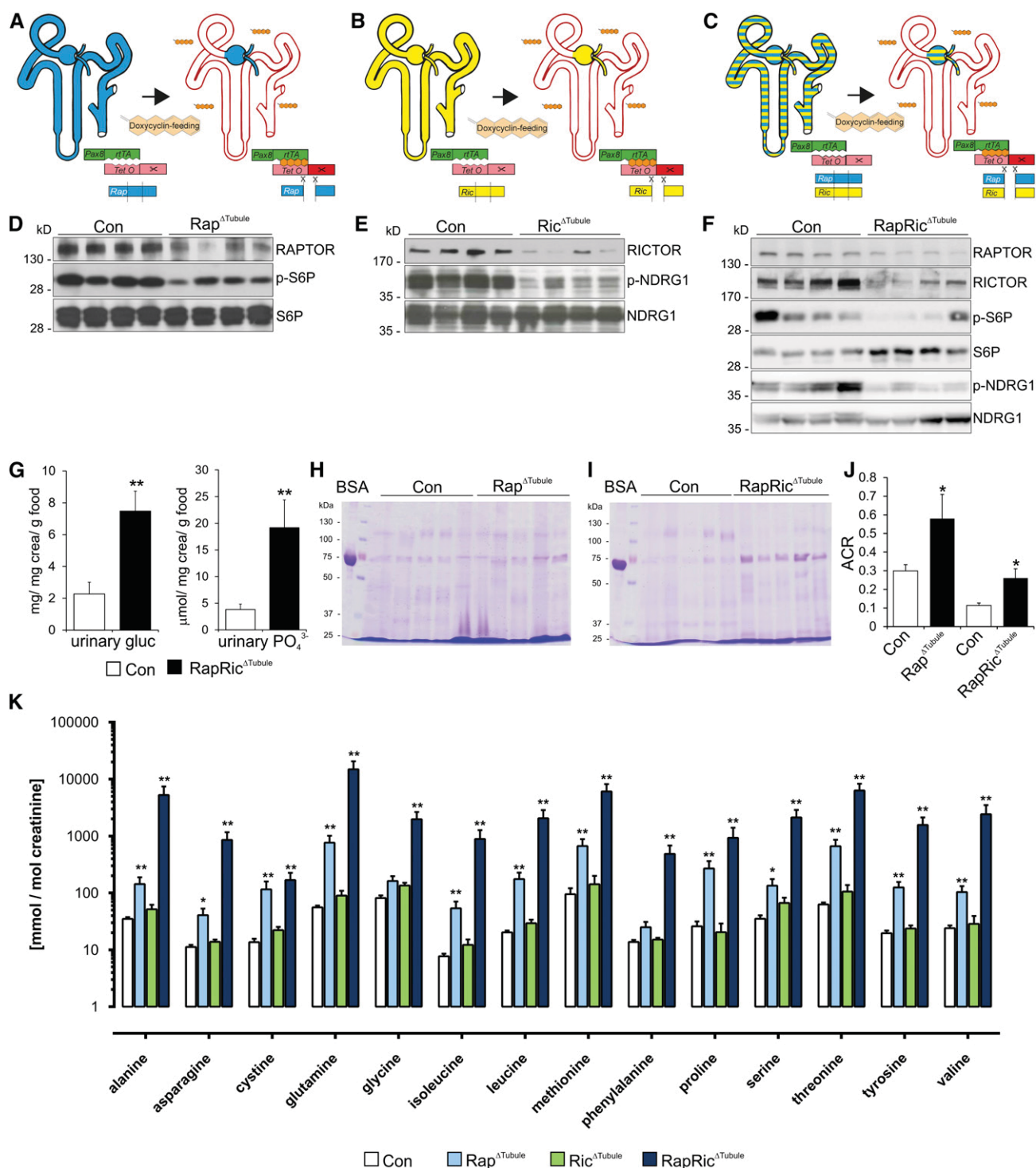
Figure 1. Proximal tubular deletion of mTORC1 leads to a Fanconi like syndrome. (A–C) Schematic of recombination strategy and site of inducible *Pax8rtTA* × *TetOCre*–mediated (A) *Raptor*, (B) *Rictor*, and (C) double knockout within the tubular system. (D–F) Demonstration of knockout efficacy by Western blot of (D) RAPTOR and downstream target p-S6P/S6P in Rap$^{\Delta Tubule}$, (E) RICTOR and the downstream target p-NDRG1/NDRG1 in Ric$^{\Delta Tubule}$, and (F) RAPTOR and RICTOR and downstream targets p-S6P/S6P and p-NDRG1/NDRG1 in RapRic$^{\Delta Tubule}$. (G) Urinary glucose (gluc) and phosphate (PO$_4^{3-}$) excretions in RapRic$^{\Delta Tubule}$ were increased. (H and I) Coomassie staining of SDS-PAGE prepared from urine samples loaded after normalization to urinary creatinine concentration from (H) Rap$^{\Delta Tubule}$ and (I) RapRic$^{\Delta Tubule}$. (J) Urinary albumin excretion of Rap$^{\Delta Tubule}$ and RapRic$^{\Delta Tubule}$. (K) Urinary neutral amino acid excretion of Rap$^{\Delta Tubule}$, Ric$^{\Delta Tubule}$, and RapRic$^{\Delta Tubule}$. ACR, albumin-creatinine-ratio; Con, control; crea, creatinine. *P value versus control <0.05; **P value versus control <0.01.
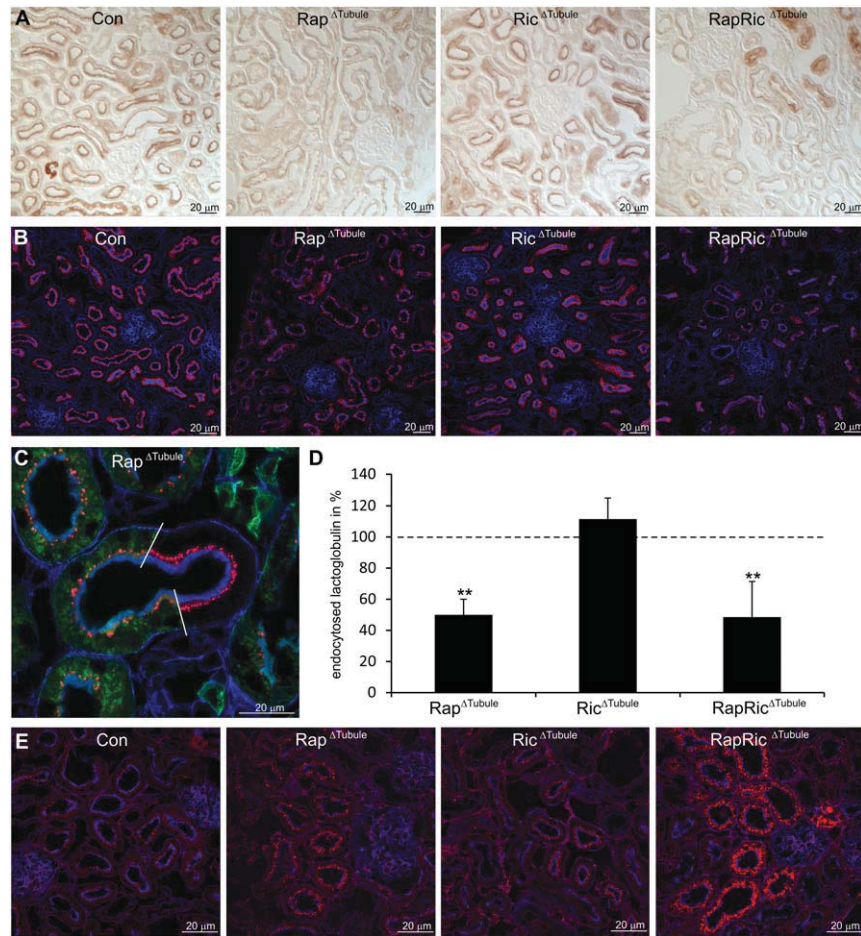
Figure 2. Deletion of mTORC1 leads to a reduced fluid-phase as well as receptor-mediated endocytosis and blocks intracellular trafficking. (A) Fluid-phase and (B) receptor-mediated endocytosis is shown by the uptake of horseradish peroxidase or Alexa555-coupled lactoglobulin (red stain), respectively, injected 5 minutes before perfusion-fixation. Reduced uptake is found in Rap$^{\Delta Tubule}$ and RapRic$^{\Delta Tubule}$. (C) Cell by cell analysis of receptor-mediated endocytosis in Rap$^{\Delta Tubule}$ × *mT/mG* mice. *Cre*-positive cells (green stain) show reduced endocytic uptake of Alexa555-coupled lactoglobulin (red vesicular staining) in comparison with *Cre*-deficient cells. (D) Quantification of Alexa555-coupled lactoglobulin of Rap$^{\Delta Tubule}$, Ric$^{\Delta Tubule}$, and RapRic$^{\Delta Tubule}$ normalized to the respective control mice. Significantly reduced uptake is shown for Rap$^{\Delta Tubule}$ and RapRic$^{\Delta Tubule}$ animals. (E) Assessment of endogenous albumin content in Rap$^{\Delta Tubule}$, Ric$^{\Delta Tubule}$, and RapRic$^{\Delta Tubule}$. Note the increased number and size of albumin-containing vesicles. In immunofluorescence images, kidney sections were counterstained with Alexa647 phalloidin (blue stain) to mark actin filaments of the BBM. Con, control. Scale bar, 20 μm. **$P<0.01$.

with respective control animals (Figure 2B). Introducing an *mT/mG* reporter allele into Rap$^{\Delta Tubule}$ animals revealed very few events of a mosaic *Cre* expression in PT cells. However, these few mosaic areas allowed a detailed cell to cell analysis of endocytosis. *Cre*–positive, *Raptor*–deficient cells in comparison with *Cre*–negative, *Raptor*–positive cells showed a highly impaired receptor–mediated endocytosis as identified by reduced uptake of Alexa555 lactoglobulin (Figure 2C). To quantify receptor–mediated endocytotic flux, fluorimetric measurements of endocytosed Alexa555 lactoglobulin in tissue homogenates were performed. Reduced endocytotic fluxes were observed in Rap$^{\Delta Tubule}$ and RapRic$^{\Delta Tubule}$ animals, with no difference in Ric$^{\Delta Tubule}$ mice (Figure 2D). To examine intracellular trafficking, we stained for cellular endogenous albumin distribution.

Rap$^{\Delta Tubule}$ mice and even more RapRic$^{\Delta Tubule}$ mice showed an accumulation of endogenous albumin with increases in vesicle size and number (Figure 2E). This is in agreement with reduced intracellular trafficking and protein processing. Because MEGALIN and CUBILIN are the main receptors for PT endocytosis, their expression pattern and abundance were analyzed. Immunoblotting and staining analyses revealed no change between groups in either subcellular localization or expression level (Supplemental Figure 3).

Taken together, these data show that mTOR function is required for PT endocytosis and intracellular trafficking, whereas the abundance of the apical scavenger receptors seemed unaffected. To analyze whether duration of kinase deletion could play a role, we assessed histologic alterations in

Rap$^{\Delta Tubule}$ and RapRic$^{\Delta Tubule}$ mice 3 months after induction. In Rap$^{\Delta Tubule}$ and RapRic$^{\Delta Tubule}$ (much stronger) animals, the renal cortex was reduced, which was mainly caused by shrinkage of the convoluted part of the PT (Supplemental Figure 4A). MEGALIN and CUBILIN expression levels remained unaltered in Rap$^{\Delta Tubule}$ but were decreased in RapRic$^{\Delta Tubule}$ (Supplemental Figure 4, B and C). We next analyzed the expression pattern of the Na$^+$/K$^+$-ATPase (NKA), a basolateral protein being expressed in a polarized fashion. Interestingly, in Rap$^{\Delta Tubule}$ and RapRic$^{\Delta Tubule}$ animals 3 months postinduction, apical NKA–containing vesicles were observed, showing an apical mis-sorting of this protein. In addition, we discerned a striking reduction of basolateral NKA expression in RapRic$^{\Delta Tubule}$ animals. These data show that apical scavenger receptor expression remained intact in Rap$^{\Delta Tubule}$ mice, although signs of epithelial depolarization could be detected, whereas PT cells dedifferentiated in RapRic$^{\Delta Tubule}$ animals, leading to reduced MEGALIN and CUBILIN expression.

Loss of mTOR Results in Altered Apical Plasma Membrane Topology with a Reduced Reabsorption Surface *In Vivo*

Light and electron microscopy analyses were performed to correlate reduced PT function with changes in morphology. Periodic acid–Schiff staining on paraffin sections revealed reduced brush border membrane (BBM) microvilli in all transgenic knockout mice, which was most evident in Rap$^{\Delta Tubule}$ and RapRic$^{\Delta Tubule}$ compared with control animals (Figure 3A). The overall gross morphology, however, remained unchanged as shown in methylene blue–stained semithin sections (Figure 3B). Subcellular electron microscopy analysis of PT S1 segments in Rap$^{\Delta Tubule}$ and RapRic$^{\Delta Tubule}$ mice showed reduced microvilli length and endosomal vesicle formation compared with control animals as well as reduced numbers of mitochondria in RapRic$^{\Delta Tubule}$ animals (Figure 3C, Supplemental Table 2). Additionally, largely inflated early and late endosomes and Golgi cisternae were observed in Rap$^{\Delta Tubule}$ and RapRic$^{\Delta Tubule}$ mice.

Reduced Endocytosis Is Caused by Diminished Formation of Clathrin-Coated Vesicles

To gain additional mechanistic insights, we analyzed endocytosis in the well established opossum kidney proximal tubule cell (OKC) line.[17] OKCs were incubated with 100 nM rapamycin (mTORC1 inhibitor), 100 nM PP242 (mTORC1+2 inhibitor), or 250 nM torin (mTORC1+2 inhibitor) for 3 days or 3 or 10 μM PF-4708671 (S6K1 inhibitor) overnight before endocytosis assays followed by flow cytometric analysis of endocytosed Alexa647 albumin. Similar to our *in vivo* findings, treatment with rapamycin, PF-4708671, PP242, or torin led to a strong reduction of endocytosed Alexa647 albumin (Supplemental Figure 5A). Increasing concentrations of rapamycin reduced the endocytosis rate in a concentration-dependent manner (Supplemental Figure 5B). To allow specific differentiation between mTORC1 and mTORC2 signaling, we performed shRNA–mediated viral knockdown of the main mTORC1–dependent translational regulator *S6K1*, *RICTOR*, or both genes together. Compared with mock transduction, all virally transduced OKCs showed a significant reduction in their endocytosis rate, with the strongest decrease observed in S6K1 or S6K1/RICTOR shRNA knockdown (Supplemental Figure 5, C and D). mTORC1 and mTORC2 signaling showed no influence on lysosomal pH and enzyme activity (Supplemental Figure 5E). In addition, enzymatic activity of galactosidase, mannosidase, and α-glucuronidase remained unchanged on viral knockdown of S6K1, RICTOR, or S6K1/RICTOR compared with mock transduction (data not shown). Formation of clathrin-coated vesicles as a readout of membrane formation was reduced in S6K1 and double shRNA–transduced OKCs (Supplemental Figure 5, F and G). This may affect the formation of endocytotic vesicles as described in the electron microscopic analysis of the transgenic mouse models.

Proteomic and Phosphoproteomic Analyses of Kidney Cortex Identify a Putative mTOR–Dependent Transport Regulatory Protein Network

To further elucidate the molecular causes for the observed reduction in PT transport function, we performed detailed proteomic and phosphoproteomic analyses of renal cortex in Rap$^{\Delta Tubule}$ and respective control animals. Although overall differences between control and Rap$^{\Delta Tubule}$ animals were rather subtle (Figure 4A), several amino acid transporters, such as SLC6A19 (B^{0}AT1), SLC7A7 (y$^+$LAT1), and SLC3A2 (4F2*hc*), as well as proteins related to polarity and endocytosis (*e.g.*, DOCK8, Bcl2-like 1 [BCL-x$_L$], Ras–related protein Rab-10 [RAB10], and sorting nexin 8 [SNX8]) were reduced (Figure 4B, Supplemental Table 3). Making use of the mosaic expression pattern of RAPTOR-deficient cells in Rap$^{\Delta Tubule}$, we could confirm by immunohistochemistry the reduced expression of B^{0}AT1, y$^+$LAT1, 4F2*hc*, DOCK8, and BCL-x$_L$ in RAPTOR-deficient cells in comparison with wild-type cells (Figure 5, A–E). This was corroborated by Western blot analysis from isolated cortical kidney membranes (Figure 5F), which confirmed our proteomic findings.

Interestingly, BBM-bound enzymes, such as 5′ nucleotidase, glutamylaminopeptidase, and angiotensin-converting enzyme 2, or mitochondrial proteins, such as cytochrome P450 4A12A and cytochrome b-c1 complex subunit 8, were upregulated, likely in a compensatory fashion in Rap$^{\Delta Tubule}$ mice (Figure 4B). We carried out gene ontology enrichment of the changed protein population compared with the unchanged protein population. Several nutrient transport pathways in the PT were again found to be significantly downregulated in Rap$^{\Delta Tubule}$ mice (Figure 4C). Small filtered proteins taken up by the PT (*e.g.*, transthyretin, angiotensinogen, retinol binding protein, vitamin D binding protein, and β2-microglobulin) were enriched in the renal cortexes of Rap$^{\Delta Tubule}$ animals compared with controls (Figure 4D, Supplemental Table 3). Overall analysis of phosphosites again only showed subtle
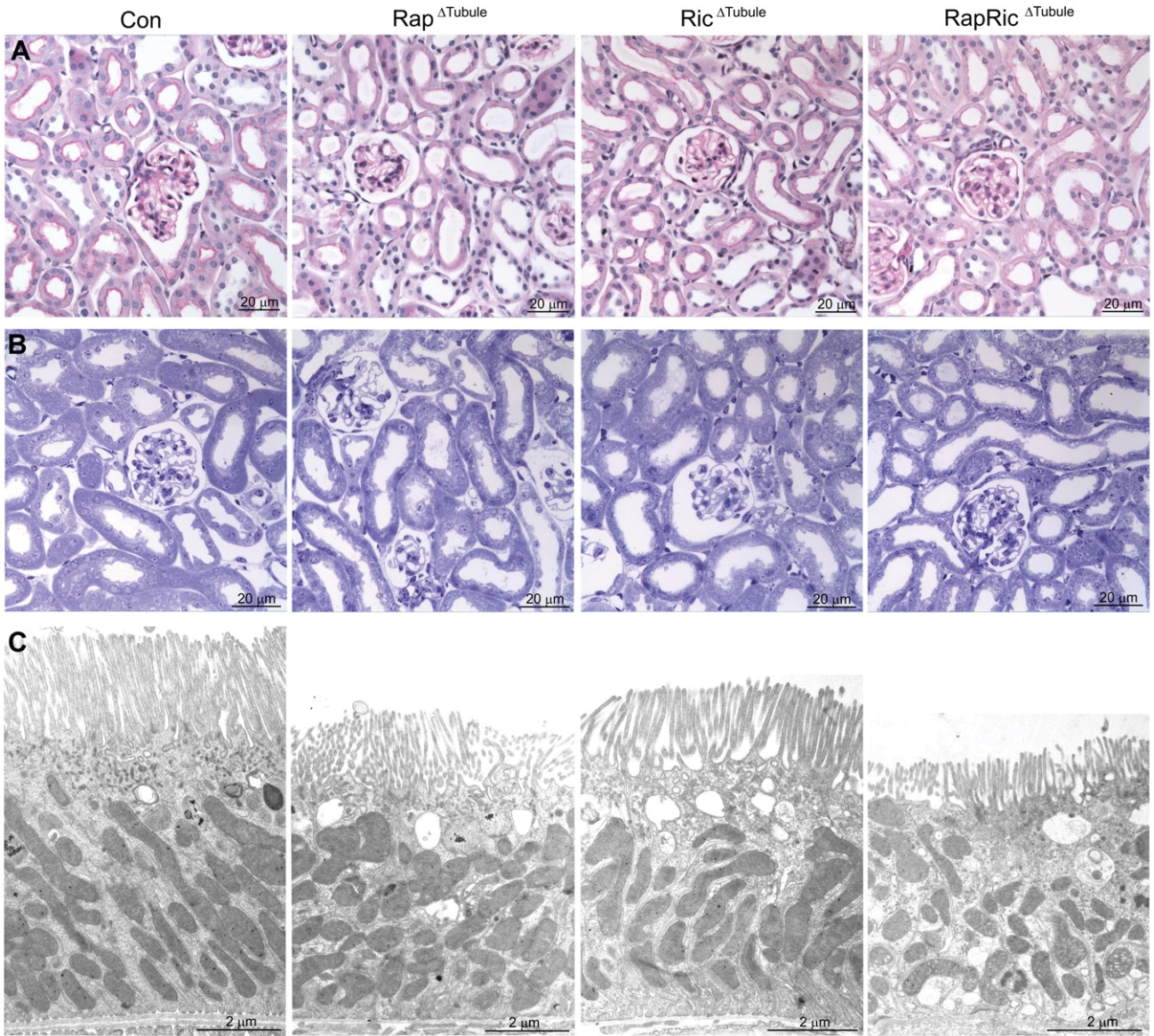
Figure 3. mTOR deletion leads to ultrastructural alterations in PT cells. (A) Periodic acid–Schiff–stained sections of control (Con), Rap$^{\Delta Tubule}$, Ric$^{\Delta Tubule}$, and RapRic$^{\Delta Tubule}$ showing reduced BBM length in mutants compared with control mice. (B) Semithin sections counterstained with methylene blue from Con, Rap$^{\Delta Tubule}$, Ric$^{\Delta Tubule}$, and RapRic$^{\Delta Tubule}$ showing intact morphology of epithelial cells. (C) Electron microscopy images of Con, Rap$^{\Delta Tubule}$, Ric$^{\Delta Tubule}$, and RapRic$^{\Delta Tubule}$ showing reduced number and length of BBM microvilli and reduced number of clathrin-coated vesicles as well as recycling endosomes in otherwise normal cellular structures in mutant compared with control animals. Note the increase in early and late endosomes in mutant cells compared with Con in C. Scale bar, 20 μm and 2 μm.

differences between the two genotypes (Figure 4E). However, detailed analysis revealed reduced phosphorylation of several transport proteins, especially amino acid transporter SLC7A9 (b$^{0,+}$AT) and the sodium–dependent glucose transporter 2 (SGLT2; SLC5A2) providing additional potential molecular explanation for the observed aminoaciduria and glucosuria (Figure 4F, Supplemental Table 4). Additionally, an up to eight times reduction on three so far unknown phosphosites of the Na^{+}/HCO$_3^{-}$ cotransporter (NBC1; T3, S232, and S1060) and the ArfGEF GBF-1 (S179) were identified. To further evaluate the functional importance of the later protein, we used the

Drosophila melanogaster system to perform an siRNA knockdown in nephrocytes, the highly endocytotic storage kidney cells of the fly. Interestingly, knockdown of GBF-1 led to a marked reduction in endogenous uptake of a fluorescently labeled marker protein (Figure 5G). In line, TEM showed a phenotype consistent with a severely deranged endocytotic machinery (Figure 5H).

In contrast, several mTORC2 targets, especially NDRG1, were found to have an increased phosphorylation status (T328 and S342). Similar to the gene ontology enrichment analysis on protein level, transmembrane transport activity as well as
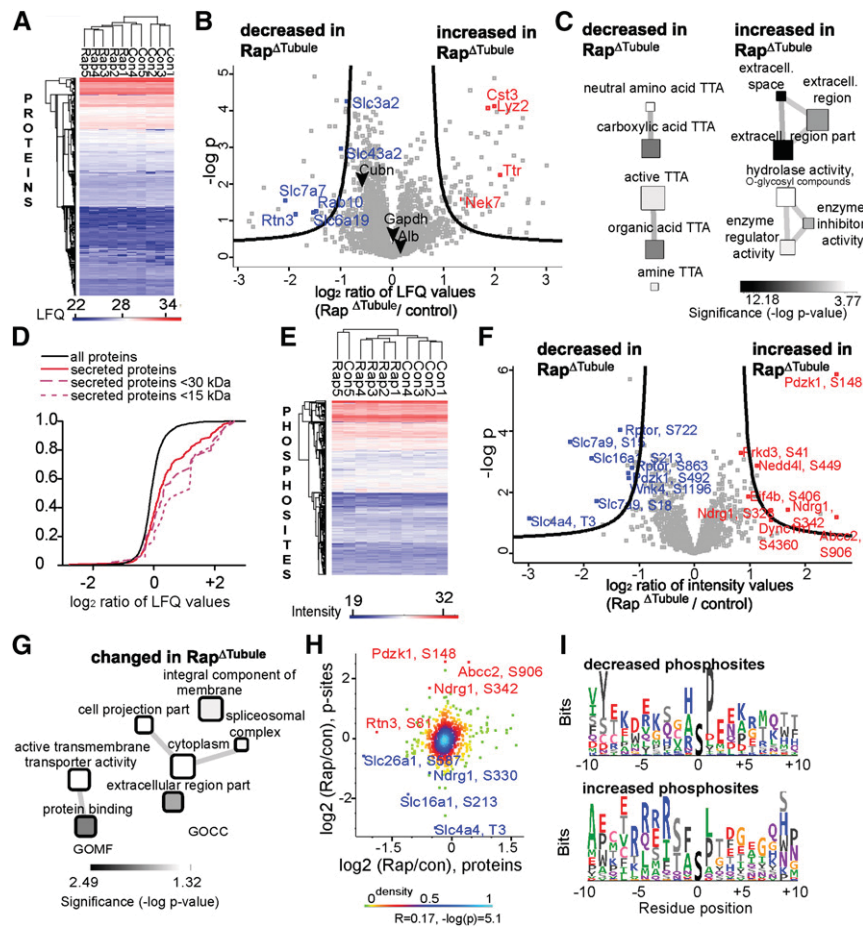
Figure 4. Proteomic analyses of Rap$^{\Delta Tubule}$ mice shows reduced abundance and phosphorylation of both tubular transport proteins and regulators of endocytosis. (A) Hierarchical clustering of identified proteins and the samples on the basis of the protein LFQ intensities. (B) Volcano plot of the proteomic analysis of Rap$^{\Delta Tubule}$ mice compared with the control mice. Proteins beyond the curved lines were considered to be significantly changed (red, increased; blue, decreased). (C) Analysis of over–represented gene ontology (GO) terms in the decreased and increased protein populations compared with the unchanged protein population (Fisher exact test; size of the squares represents number of condensed terms). (D) Cumulative histogram of all quantified proteins (black) and proteins with the uniprot keyword secreted (red). Subgroups of this protein population with small molecular weight are depicted in magenta. (E) Hierarchical clustering of identified phosphorylation site intensity. (F) Volcano plot of the intensity of phosphorylation sites in the Rap$^{\Delta Tubule}$ mice compared with the control mice. Phosphorylation sites beyond the curved lines were considered to be significantly changed. (G) Analysis of over–represented GO terms in the significantly changed phosphorylation site population compared with the unchanged population (Fisher exact test). (H) Comparison of logarithmized expression ratios (Rap$^{\Delta Tubule}$ to control) for proteins and their respective phosphorylation sites. Density is color coded. (I) Position-weighted matrix of phosphorylation motifs present in the increased and decreased phosphorylation site populations. GOCC, go-term cellular component; GOMF: go-term molecular function; LFQ, label free quantification; TTA: trans-tubular-absorption.

membrane components were most significantly regulated (Figure 4G). Interestingly, when integrating both proteomic and phosphoproteomic datasets, it became evident that changes in phosphorylation were not a mere consequence of changes in protein abundance (Figure 4H). We finally analyzed phosphomotifs being up- or downregulated. Downregulated phosphorylation sites mainly contained a proline-directed motif ([S/T]–P), a motif consistent with phosphorylation by mTOR but also, other proline–directed kinases (Figure 4I).[18] Phosphorylation sites containing the AGC Kinase motif RxxS were increased.

DISCUSSION

Although the pleiotropic functions of mTOR kinases have recently become evident, very little is known about their complex role in regulating epithelial protein transport and endocytosis. Interestingly, registry datasets after renal transplantation document reduced serum potassium and phosphorus levels in sirolimus-treated patients,[19–21] pointing toward an mTOR regulatory function for electrolyte transport and homeostasis. Using inducible, gene–targeted, specific disruption of mTORC1, mTORC2, or both mTOR complexes in
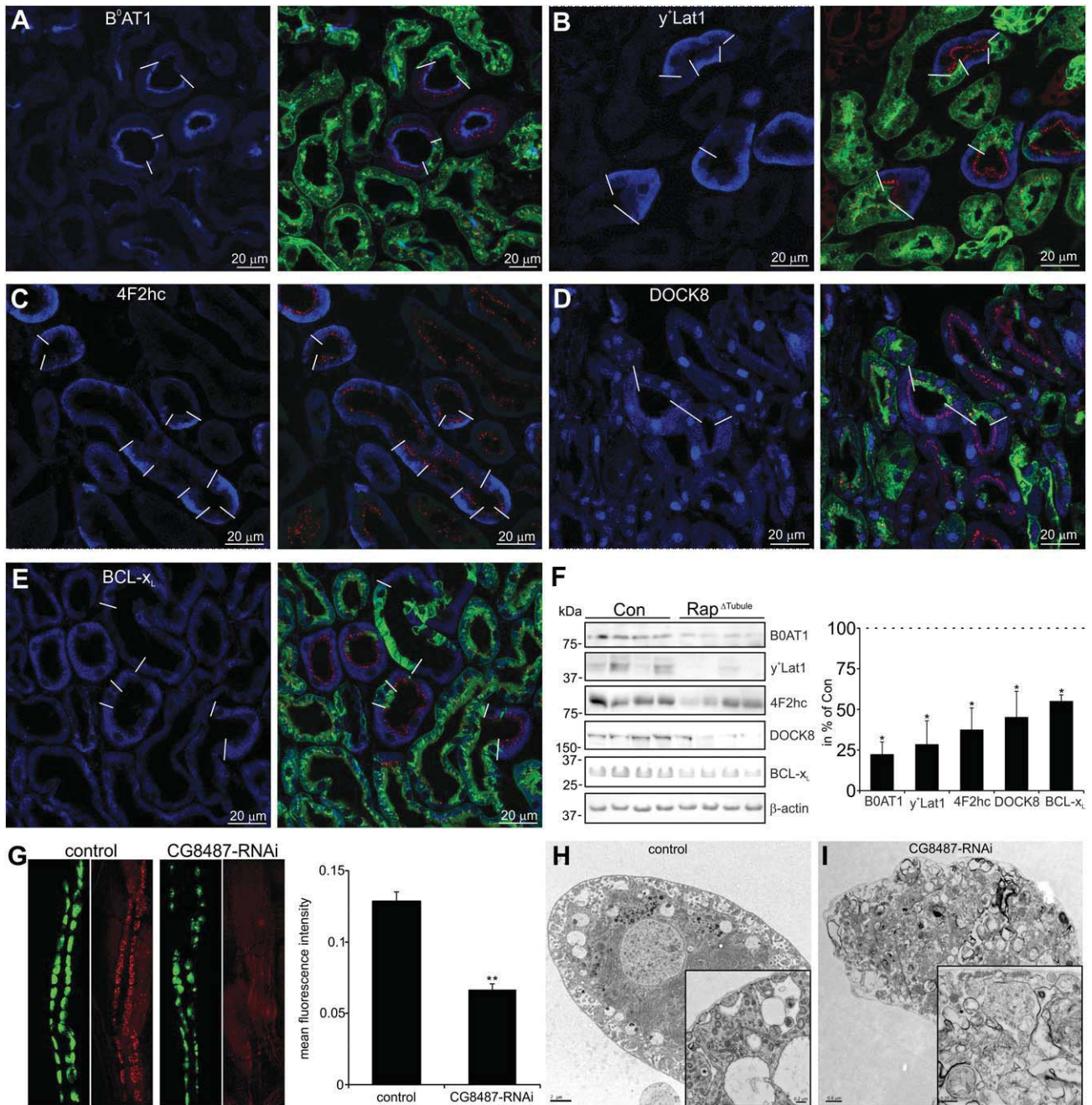
Figure 5. Reduced expression of transport proteins and regulators of endocytosis can be found in proximal tubular cells of Rap$^{\Delta Tubule}$ mice. For better illustration, Rap$^{\Delta Tubule} \times mT/mG$ mice were used for analysis of expression levels of various proteins by cell to cell analysis of Cre-positive (green stain) compared with wild-type cells. (A) B^{0}AT1, (B) y$^+$Lat1, (D) DOCK8, and (E) BCL-x$_L$ showed strongly reduced expression levels in Cre-positive cells compared with wild-type cells. Borders between cells types are marked with white bars. (C) In the case of 4F2*hc*, Alexa555 lactoglobulin was used to distinguish between Cre-positive cells and wild-type cells, and borders are marked by white bars. Cre-positive cells with reduced uptake of Alexa555 lactoglobulin also showed reduced basolateral expression level of 4F2*hc*. (F) Western blots of B^{0}AT1, y$^+$Lat1, 4F2*hc*, DOCK8, and BCL-x$_L$ from control (Con) and Rap$^{\Delta Tubule}$ (left panel) and densitometric evaluation (right panel) confirm immunohistochemical results. (G) RNAi-mediated knockdown of Gbf-1 (CG8487; gartenzwerg) was generated in *Drosophila*, and RFP-ANP (red) fluorescence uptake was measured in nephrocytes (green). Quantification is presented in right panel. (H and I) Transmission electron microscopy images of *Drosophila* from (H) control and (I) Gbf-1 knockdown are shown. In comparison with control nephrocytes with a proper formation of the endocytotic machinery, Gbf-1 knockdown shows loss of clathrin vesicles and early, late, and recycling endolysomes, whereas the formation of aberrant vesicular structures is increased. Scale bar, 20 μm in A–E; 2 μm in H; 0.2 μm in H, inset; 0.5 μm in I; 0.25 μm in I, inset. *P value versus control <0.05; **P value versus control <0.01. RFP-ANP, red-fluorescent-protein atrial natriuretic peptide; RNAi, RNA interference.

PT cells, we can now delineate the influence of mTOR signaling on PT physiology, protein transport, and endocytosis with unprecedented detail (Figure 6). In fact, disruption of mTORC1 signaling leads to a Fanconi-like syndrome, which presents with phosphaturia, glucosuria, aminoaciduria, and LMW proteinuria. On a molecular level, both fluid-phase and receptor–mediated endocytosis are impaired and coincide with an altered BBM length and vesicle formation in the PT.

mTOR Regulates the Endocytosis Machinery in PT Epithelial Cells

Tubular albuminuria and LMW proteinuria are well established features of Fanconi syndrome and known to occur in patients treated with mTOR inhibitors after renal transplantation.[22,23] Our study now highlights a significantly reduced tubular internalization in Rap$^{\Delta Tubule}$ and RapRic$^{\Delta Tubule}$ mice, which was consistent with endocytosis assays performed *in vitro*. Surprisingly, MEGALIN and CUBILIN, which are the main renal scavenger receptors for filtered urinary proteins, were not directly regulated by mTOR in our functional studies (short–term follow-up after induced mTOR deletion).[9] This is in contrast to recently published data, in which long–term (6 months) rapamycin treatment was shown to lead to a reduced MEGALIN expression in mice.[24] However, it has been recognized that long-term administration of rapamycin in high doses additionally inhibits mTORC2 and exerts cytotoxic effects.[25] In agreement, long–term follow-up studies (3 months) in our double–knockout RapRic$^{\Delta Tubule}$ mice showed a reduced MEGALIN expression, whereas Rap$^{\Delta Tubule}$ mice maintained a stable MEGALIN expression. Additionally, we detected a strong reduction in the overall renal cortex volume because of shortening of the S1/2 segment in Rap$^{\Delta Tubule}$ mice, and it was more pronounced in RapRic$^{\Delta Tubule}$ mice, confirming the importance of mTOR signaling for general cellular programs, such as cell growth, proliferation, and metabolism.

In addition to the impairment of the initiating steps of endocytosis, we also observed a disturbed endocytic trafficking as indicated by increased amounts of endocytosed albumin in Rap$^{\Delta Tubule}$ and RapRic$^{\Delta Tubule}$ animals. Furthermore, proteomic analysis of Rap$^{\Delta Tubule}$ identified increased intracellular amounts of LMW proteins, such as angiotensinogen, retinol binding protein, vitamin D binding protein, and β2-microglobulin. These proteins are physiologically endocytosed by PT cells and further processed for degradation or transcytosis.[26] Intracellular trafficking is a prerequisite for both processes, and its disturbances may, hence, lead to intracellular accumulations as observed in our animal models (Figure 2).

Proteomic data of Rap$^{\Delta Tubule}$ kidney cortex did identify reduced expression or phosphorylation level of interesting candidate proteins, such as BCL-x$_L$, GBF-1, SNX8, RAB10, and DOCK8, to explain the reduced endocytosis rate, altered apical membrane differentiation, and impaired intracellular trafficking. BCL-x$_L$ is an antiapoptotic protein with a role in the regulation of membrane dynamics and endocytosis.[27]

DOCK8, a member of the evolutionarily conserved DOCK family proteins,[28] was shown to bind to nucleotide-free CDC42 to mediate the GTP-GDP exchange reaction. Thereby, CDC42 is spatially activated at the plasma membrane,[29] where it plays a crucial role in apical differentiation and BBM formation.[30] Another GEF, the ArfGEF GBF-1, presented a strongly diminished phosphorylation status in Rap$^{\Delta Tubule}$ animals. Arf-GEFs are nucleotide exchange factors for Arf GTPases, which have diverse functions in vesicle coat formation and vesicle-cytoskeleton interactions.[31] SNX8 was found to localize at early endosomes, and its knockdown was shown to affect intracellular vesicle trafficking.[32] RAB10 has been localized to many organelles, such as endoplasmic reticulum (ER), Golgi, early endosomes, and recycling endosomes, and mediates membrane trafficking within the cell partly by regulating endosomal phosphatidylinositol-4,5-bisphosphate levels.[33,34] Together, these data reveal a novel theme of mTOR function by regulating a series of proteins being specifically involved in endocytosis and vesicle transport.

mTOR Regulates Specific Apical Tubular Transport Proteins

Many BBM transporters were affected by *Raptor* deletion, resulting in a Fanconi-like syndrome. SGLT2 (SLC5A2) is the main apical glucose transporter in the PT S1 and S2 segments, with an exclusive localization to the BBM.[35] The transporter activity is decisively regulated by phosphorylation.[36] Phosphoproteomics of Rap$^{\Delta Tubule}$ mice pointed to a reduced phosphorylation of SGLT2 at S623 in comparison with control animals. This residue is a highly conserved phosphosite between species, including human SGLT2 (S624).[36] Augmented phosphorylation at this site was shown to enhance glucose transport by increasing membrane insertion of SGLT2.[36] Loss of mTORC1-induced phosphorylation at S623 could, hence, contribute to glucosuria in Rap$^{\Delta Tubule}$ and RapRic$^{\Delta Tubule}$ animals.

Rap$^{\Delta Tubule}$ and even more so, RapRic$^{\Delta Tubule}$ mice displayed a highly increased excretion of neutral, basic, and acidic amino acids compared with control mice (Figure 1, Supplemental Figure 2). Proteomic and phosphoproteomic analyses of Rap$^{\Delta Tubule}$ animals identified reduced expression or phosphorylation states of many amino acid transporters known to be highly expressed in the PT.[37] Among these, SLC6A19 (B^{0}AT1), SLC7A7 (y$^+$LAT1), and SLC3A2 (4F2*hc*) had reduced expression levels, whereas diminished phosphorylation was found in SLC7A9 (b$^{0,+}$AT) at position S15 and S18. B^{0}AT1 mediates neutral amino acid transport from the luminal compartment into the cellular lumen.[37] b$^{0,+}$AT, a member of the heterodimeric amino acid transporter family, is the light subunit of SLC3A1 (rBAT), facilitating dibasic amino acid and cysteine transport into the cell. y$^+$LAT1, another member of the heterodimeric amino acid transporter family, is exclusively expressed in the PT, whereas its companion 4F2*hc* is ubiquitously expressed. y$^+$LAT1 and 4F2*hc* both assemble to form a heterodimeric amino acid transporter localizing to
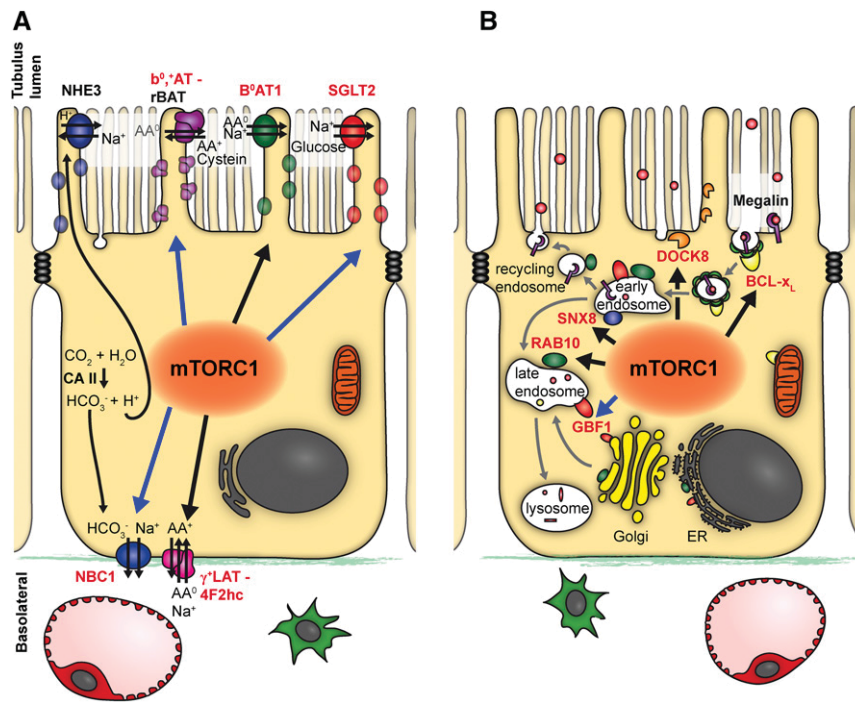
Figure 6. Putative mTORC1–dependent regulation of proximal tubular transport and endocytosis. (A) mTORC1 seems to regulate apical and basolateral PT transport proteins. mTORC1 could directly phosphorylates SGLT2 and NBC1 to increase reabsorption of glucose and sodium and excretion of sodium and bicarbonate. mTORC1 might positively influence the expression level of the amino acid transporter B^{0}AT1 and y$^+$LAT-4F2hc and the phosphorylation status of b$^{0,+}$AT1-rBAT to reabsorb filtered amino acids and secrete them into the bloodstream. (B) mTORC1 could regulate PT endocytosis, membrane biogenesis, vesicle trafficking, and cell polarity. mTORC1 likely controls apical membrane biogenesis and cell polarity by affecting expression level of DOCK8, apical clathrin–coated pit and vesicle formation, and endocytosis by affecting the expression levels of BCL-x$_L$, SNX8, and RAB10 and phosphorylation level of GBF-1. Also, it controls proper endoplasmic reticulum (ER) function and Golgi integrity again by influencing the expressions and phosphorylation levels of RAB10 and GBF-1, respectively.

the basolateral membrane of the PT predominantly in the S1 segment. Interestingly, this transporter mediates efflux of di-basic amino acids in exchange for neutral amino acids and sodium together with b$^{0,+}$AT and its subunit rBAT. Loss of function mutations result in an inefficient urea cycle with consecutive hyperammonemia,[37] which could, at least in part, explain increased urea values of RapRic$^{\Delta Tubule}$ animals.

Phosphoproteomic analysis of Rap$^{\Delta Tubule}$ renal cortexes revealed a strong reduction in the phosphorylation level of three phosphorylation sites on SLC4A4 (NBC1). Inactivating mutations of this gene were reported to lead to renal PT acidosis, another commonly observed feature of Fanconi syndrome.[6] Whether the identified phosphosites influence NBC1 transport needs additional determination on a molecular level.[38,39] In accordance with other reports using rapamycin, despite similar expression of the major PT phosphate transporters (NaPi-IIa, NaPi-IIc, and Pit-2), we detected phosphaturia in Rap$^{\Delta Tubule}$ and RapRic$^{\Delta Tubule}$ animals.[40,41] Influence of mTORC1 on so far unidentified interaction partners might be responsible for this enigmatic finding.

In summary, mTORC1 deletion leads to a generalized PT dysfunction, mimicking the clinical diagnosis of Fanconi syndrome (Figure 6). Our in-depth analysis reveals probable molecular pathways being affected in an organ-specific fashion. Additionally, we have identified a novel main kinase regulator of PT function, opening new avenues for subsequent studies to unravel the kinase networks governing PT transport in health and disease.

CONCISE METHODS

Animals and Treatments

All animal experiments were conducted according to the National Institutes of Health guide for the care and use of laboratory animals as well as the German law for the welfare of animals, and they were approved by local authorities (G-13/07, M-9/11, and M-4/13). Mice were housed in an SPF facility with free access to chow and water and a 12-hour day-night cycle. Breeding and genotyping were done according to standard procedures. *Raptorfl/fl* and *Rictorfl/fl* mice have been described previously[42] and were crossed to *Pax8rtTA*[43] and *TetOCre*[44] animals. At 5 weeks of age, inducible animals and respective controls (lacking either *TetOCre* or *Pax8rtTA*) received doxycycline hydrochloride (Fagron, Barsbuettel, Germany) *via* the

drinking water (2 mg/ml with 5% sucrose protected from light) for a total of 14 days. To estimate recombination efficacy and identify cellular mosaicisms, we crossed the reporter mouse strain *mT/mG* with some *Raptorfl/fl* × *Pax8rtTA* × *TetOCre* mice (Supplemental Material).[45]

Presentation of Data and Statistical Analyses

Quantitative data are presented as means±SEM. Statistical comparisons were performed using the GraphPad Prism Software Package 6 (GraphPad Software, La Jolla, CA). For statistical comparison, the Mann–Whitney *U* test, the two–tailed *t* test, and where appropriate, ANOVA were used. *P* values of <0.05 were considered statistically significant.

DISCLOSURES

None.

REFERENCES

1. Smith HW: From Fish to Philosopher, Boston, Little, Brown, 1953
2. Zhuo JL, Li XC: Proximal nephron. *Compr Physiol* 3: 1079–1123, 2013
3. Makrides V, Camargo SM, Verrey F: Transport of amino acids in the kidney. *Compr Physiol* 4: 367–403, 2014
4. Wagner CA, Rubio-Aliaga I, Biber J, Hernando N: Genetic diseases of renal phosphate handling. *Nephrol Dial Transplant* 29[Suppl 4]: iv45–iv54, 2014
5. Klootwijk ED, Reichold M, Helip-Wooley A, Tolaymat A, Broeker C, Robinette SL, Reinders J, Peindl D, Renner K, Eberhart K, Assmann N, Oefner PJ, Dettmer K, Sterner C, Schroeder J, Zorger N, Witzgall R, Reinhold SW, Stanescu HC, Bockenhauer D, Jaureguiberry G, Courtneidge H, Hall AM, Wijeyesekera AD, Holmes E, Nicholson JK, O'Brien K, Bernardini I, Krasnewich DM, Arcos-Burgos M, Izumi Y, Nonoguchi H, Jia Y, Reddy JK, Ilyas M, Unwin RJ, Gahl WA, Warth R, Kleta R: Mistargeting of peroxisomal EHHADH and inherited renal Fanconi's syndrome. *N Engl J Med* 370: 129–138, 2014
6. Klootwijk ED, Reichold M, Unwin RJ, Kleta R, Warth R, Bockenhauer D: Renal Fanconi syndrome: Taking a proximal look at the nephron. *Nephrol Dial Transplant* 30: 1456–1460, 2015
7. Fanconi G: Der frühinfantile nephrotisch-glykosurische Zwergwuchs und hypophosphatämische Rachiti. *Jahrbuch der Kinderheilkunde* 147: 299, 1936
8. Christensen EI, Birn H, Storm T, Weyer K, Nielsen R: Endocytic receptors in the renal proximal tubule. *Physiology (Bethesda)* 27: 223–236, 2012
9. Christensen EI, Verroust PJ, Nielsen R: Receptor-mediated endocytosis in renal proximal tubule. *Pflugers Arch* 458: 1039–1048, 2009
10. Grahammer F, Wanner N, Huber TB: mTOR controls kidney epithelia in health and disease. *Nephrol Dial Transplant* 29[Suppl 1]: i9–i18, 2014
11. Laplante M, Sabatini DM: mTOR signaling in growth control and disease. *Cell* 149: 274–293, 2012
12. Wullschleger S, Loewith R, Hall MN: TOR signaling in growth and metabolism. *Cell* 124: 471–484, 2006
13. Peterson TR, Sengupta SS, Harris TE, Carmack AE, Kang SA, Balderas E, Guertin DA, Madden KL, Carpenter AE, Finck BN, Sabatini DM: mTOR complex 1 regulates lipin 1 localization to control the SREBP pathway. *Cell* 146: 408–420, 2011
14. Sarbassov DD, Guertin DA, Ali SM, Sabatini DM: Phosphorylation and regulation of Akt/PKB by the rictor-mTOR complex. *Science* 307: 1098–1101, 2005
15. Ikenoue T, Inoki K, Yang Q, Zhou X, Guan KL: Essential function of TORC2 in PKC and Akt turn motif phosphorylation, maturation and signalling. *EMBO J* 27: 1919–1931, 2008
16. Rickheit G, Wartosch L, Schaffer S, Stobrawa SM, Novarino G, Weinert S, Jentsch TJ: Role of ClC-5 in renal endocytosis is unique among ClC exchangers and does not require PY-motif-dependent ubiquitylation. *J Biol Chem* 285: 17595–17603, 2010
17. Sorribas V, Markovich D, Hayes G, Stange G, Forgo J, Biber J, Murer H: Cloning of a Na/Pi cotransporter from opossum kidney cells. *J Biol Chem* 269: 6615–6621, 1994
18. Miller ML, Jensen LJ, Diella F, Jørgensen C, Tinti M, Li L, Hsiung M, Parker SA, Bordeaux J, Sicheritz-Ponten T, Olhovsky M, Pasculescu A, Alexander J, Knapp S, Blom N, Bork P, Li S, Cesareni G, Pawson T, Turk BE, Yaffe MB, Brunak S, Linding R: Linear motif atlas for phosphorylation-dependent signaling. *Sci Signal* 1: ra2, 2008
19. Golbaekdal K, Nielsen CB, Djurhuus JC, Pedersen EB: Effects of rapamycin on renal hemodynamics, water and sodium excretion, and plasma levels of angiotensin II, aldosterone, atrial natriuretic peptide, and vasopressin in pigs. *Transplantation* 58: 1153–1157, 1994
20. Morales JM, Andrés A, Dominguez-Gil B, Sierra MP, Arenas J, Delgado M, Casal MC, Rodicio L: Tubular function in patients with hypokalemia induced by sirolimus after renal transplantation. *Transplant Proc* 35[Suppl]: 154S–156S, 2003
21. Morales JM, Wramner L, Kreis H, Durand D, Campistol JM, Andres A, Arenas J, Nègre E, Burke JT, Groth CG; Sirolimus European Renal Transplant Study Group: Sirolimus does not exhibit nephrotoxicity compared to cyclosporine in renal transplant recipients. *Am J Transplant* 2: 436–442, 2002
22. Ponticelli C, Graziani G: Proteinuria after kidney transplantation. *Transpl Int* 25: 909–917, 2012
23. Oroszlán M, Bieri M, Ligeti N, Farkas A, Meier B, Marti HP, Mohacsi P: Sirolimus and everolimus reduce albumin endocytosis in proximal tubule cells via an angiotensin II-dependent pathway. *Transpl Immunol* 23: 125–132, 2010
24. Gleixner EM, Canaud G, Hermle T, Guida MC, Kretz O, Helmstädter M, Huber TB, Eimer S, Terzi F, Simons M: V-ATPase/mTOR signaling regulates megalin-mediated apical endocytosis. *Cell Reports* 8: 10–19, 2014
25. Canaud G, Bienaimé F, Viau A, Treins C, Baron W, Nguyen C, Burtin M, Berissi S, Giannakakis K, Muda AO, Zschiedrich S, Huber TB, Friedlander G, Legendre C, Pontoglio M, Pende M, Terzi F: AKT2 is essential to maintain podocyte viability and function during chronic kidney disease. *Nat Med* 19: 1288–1296, 2013
26. Pohl M, Kaminski H, Castrop H, Bader M, Himmerkus N, Bleich M, Bachmann S, Theilig F: Intrarenal renin angiotensin system revisited: Role of megalin-dependent endocytosis along the proximal nephron. *J Biol Chem* 285: 41935–41946, 2010

27. Li H, Alavian KN, Lazrove E, Mehta N, Jones A, Zhang P, Licznerski P, Graham M, Uo T, Guo J, Rahner C, Duman RS, Morrison RS, Jonas EA: A Bcl-xL-Drp1 complex regulates synaptic vesicle membrane dynamics during endocytosis. *Nat Cell Biol* 15: 773–785, 2013

28. Ruusala A, Aspenström P: Isolation and characterisation of DOCK8, a member of the DOCK180-related regulators of cell morphology. *FEBS Lett* 572: 159–166, 2004

29. Harada Y, Tanaka Y, Terasawa M, Pieczyk M, Habiro K, Katakai T, Hanawa-Suetsugu K, Kukimoto-Niino M, Nishizaki T, Shirouzu M, Duan X, Uruno T, Nishikimi A, Sanematsu F, Yokoyama S, Stein JV, Kinashi T, Fukui Y: DOCK8 is a Cdc42 activator critical for interstitial dendritic cell migration during immune responses. *Blood* 119: 4451–4461, 2012

30. Zihni C, Munro PM, Elbediwy A, Keep NH, Terry SJ, Harris J, Balda MS, Matter K: Dbl3 drives Cdc42 signaling at the apical margin to regulate junction position and apical differentiation. *J Cell Biol* 204: 111–127, 2014

31. D'Souza-Schorey C, Chavrier P: ARF proteins: Roles in membrane traffic and beyond. *Nat Rev Mol Cell Biol* 7: 347–358, 2006

32. Dyve AB, Bergan J, Utskarpen A, Sandvig K: Sorting nexin 8 regulates endosome-to-Golgi transport. *Biochem Biophys Res Commun* 390: 109–114, 2009

33. Lv P, Sheng Y, Zhao Z, Zhao W, Gu L, Xu T, Song E: Targeted disruption of Rab10 causes early embryonic lethality. *Protein Cell* 6: 463–467, 2015

34. Shi A, Grant BD: Interactions between Rab and Arf GTPases regulate endosomal phosphatidylinositol-4,5-bisphosphate during endocytic recycling. *Small GTPases* 4: 106–109, 2013

35. Sabolic I, Vrhovac I, Eror DB, Gerasimova M, Rose M, Breljak D, Ljubojevic M, Brzica H, Sebastiani A, Thal SC, Sauvant C, Kipp H, Vallon V, Koepsell H: Expression of Na+-D-glucose cotransporter SGLT2 in rodents is kidney-specific and exhibits sex and species differences. *Am J Physiol Cell Physiol* 302: C1174–C1188, 2012

36. Ghezzi C, Wright EM: Regulation of the human Na+-dependent glucose cotransporter hSGLT2. *Am J Physiol Cell Physiol* 303: C348–C354, 2012

37. Camargo SM, Bockenhauer D, Kleta R: Aminoacidurias: Clinical and molecular aspects. *Kidney Int* 73: 918–925, 2008

38. May O, Yu H, Riederer B, Manns MP, Seidler U, Bachmann O: Short-term regulation of murine colonic NBCe1-B (electrogenic Na+/HCO3(-) cotransporter) membrane expression and activity by protein kinase C. *PLoS One* 9: e92275, 2014

39. Aeder SE, Martin PM, Soh JW, Hussaini IM: PKC-eta mediates glioblastoma cell proliferation through the Akt and mTOR signaling pathways. *Oncogene* 23: 9062–9069, 2004

40. Haller M, Amatschek S, Wilflingseder J, Kainz A, Bielesz B, Pavik I, Serra A, Mohebbi N, Biber J, Wagner CA, Oberbauer R: Sirolimus induced phosphaturia is not caused by inhibition of renal apical sodium phosphate cotransporters. *PLoS One* 7: e39229, 2012

41. Kempe DS, Dërmaku-Sopjani M, Fröhlich H, Sopjani M, Umbach A, Puchchakayala G, Capasso A, Weiss F, Stübs M, Föller M, Lang F: Rapamycin-induced phosphaturia. *Nephrol Dial Transplant* 25: 2938–2944, 2010

42. Bentzinger CF, Romanino K, Cloëtta D, Lin S, Mascarenhas JB, Oliveri F, Xia J, Casanova E, Costa CF, Brink M, Zorzato F, Hall MN, Rüegg MA: Skeletal muscle-specific ablation of raptor, but not of rictor, causes metabolic changes and results in muscle dystrophy. *Cell Metab* 8: 411–424, 2008

43. Traykova-Brauch M, Schönig K, Greiner O, Miloud T, Jauch A, Bode M, Felsher DW, Glick AB, Kwiatkowski DJ, Bujard H, Horst J, von Knebel Doeberitz M, Niggli FK, Kriz W, Gröne HJ, Koesters R: An efficient and versatile system for acute and chronic modulation of renal tubular function in transgenic mice. *Nat Med* 14: 979–984, 2008

44. Eremina V, Jefferson JA, Kowalewska J, Hochster H, Haas M, Weisstuch J, Richardson C, Kopp JB, Kabir MG, Backx PH, Gerber HP, Ferrara N, Barisoni L, Alpers CE, Quaggin SE: VEGF inhibition and renal thrombotic microangiopathy. *N Engl J Med* 358: 1129–1136, 2008

45. Muzumdar MD, Tasic B, Miyamichi K, Li L, Luo L: A global double-fluorescent Cre reporter mouse. *Genesis* 45: 593–605, 2007

This article contains supplemental material